A Stochastic Methodology to Exploit Maximum Flexibility of Swimming Pool Heating Systems

Mohsen Banaei[a], Francesco D'Ettorre[a], Razgar Ebrahimy[a], S. Ali Pourmousavi[b], Emma MV Blomgren[a], Henrik Madsen[a]

[a]Technical University of Denmark, Department of Applied Mathematics and Computer Science, Copenhagen, Denmark
[b]The University of Adelaide, School of Electrical and Electronic Engineering, Adelaide, Australia

Abstract

Swimming pool heating systems are known as one of the best flexible resources in buildings. However, they can be flexible only for a certain number of hours throughout a day due to the comfort constraints of the users. In this study, a new approach is proposed to determine a group of contract hour sets to procure maximum flexibility of swimming pool heating systems supplied by heat pumps for trading in the regulation market while respecting the comfort of users. The main advantage of the contract hour sets is the certainty in response to flexibility requests. The proposed approach consists of three main steps. First, a stochastic mixed-integer linear program is proposed to find the optimal operation of a swimming pool heating system that has agreed to provide flexibility in a contract hours set. Then, a metric is proposed to evaluate the effectiveness of contract hour sets using the results obtained in the first step. Finally, an algorithm is proposed to identify a group of the most efficient contract hour sets using the calculated metric. The proposed approach is validated through comprehensive simulation studies for a summerhouse with an indoor pool heated by a heat pump. Also, a cost-benefit analysis is performed to examine the feasibility of these contract hour sets from financial viewpoint. Simulation results show that the maximum contract hours can vary from 2 to 12 hours depending on the building occupation pattern and the minimum payment to owners is between 0.03 to 0.06 (Euro/kW).

Keywords: flexibility, heat pumps, scheduling, regulation market, stochastic MILP

Acronyms

ACHN Average Contract Hour Numbers.

CHS Contract Hour Set.

EMS Energy Management System.

HP Heat Pump.

MPC Model Predictive Control.

SMILP Stochastic Mixed Integer Linear Programming.

SPHS swimming pool heating system.

Nomenclature

Indices

f Clusters

i System uncertainty scenario

s_a flexibility request uncertainty scenario at hour a

t time intervals

Sets

A,B Subsets of CHSs, where $CHS = \{A, B\}$

$A1,A2$ Subsets of set A, where $A = \{A1, A2\}$

$B1,B2$ Subsets of set B, where $B = \{B1, B2\}$

F Set of clusters

N Set of time intervals

S Set of system uncertainty scenarios

Parameters

β_t Weighting coefficient for prioritizing the violation from comfort constraints

Δt The length of each time interval (h)

$\dot{m}$ Flow rate of water (kg/s)

$\rho_{s_a}^a$ Probability of flexibility request uncertainty scenario s at hour a

ρ_i Probability of system uncertainty scenario i

C_t^i Electricity price (Euro/kWh)

c_p Specific heat capacity of water (kj/kgK)

H_o Overall heat transfer coefficient (kW/K)

K^0 CHSs' evaluating metric

M Mass of water in the swimming pool (kg)

m Mass of water in the heat exchanger (kg)

P_n Nominal power of the HP (kW)

Q_{th} Thermal power of the heating system (Kw)

$T_{ext,t}^i$ Ambient temperature at hour t

T_t^{max} Maximum water temperature at hour t

T_t^{min} Minimum water temperature at hour t

Z Number of contract hours in a CHS

Variables

$T_{t,s_a,s_b,...,s_z}^{in,i}$ Outgoing water temperature from the swimming pool

$T_{t,s_a,s_b,...,s_z}^{out,i}$ Incoming water temperature to the swimming pool

$u_{t,s_a,s_b,...,s_z}^i$ Binary decision variable for SPHS operation

$v_{t,s_a,s_b,...,s_z}^i$ Minimum necessary violation from maximum water temperature limit to avoid infeasibility.

$w_{t,s_a,s_b,...,s_z}^i$ Minimum necessary violation from minimum water temperature limit to avoid infeasibility

1. Introduction

According to the definition by International Energy Association (IEA), "power system flexibility is its ability to reliably and cost-effectively manage the variability and uncertainty of demand and supply across all relevant timescales" [1]. Flexibility is crucial for reliable operation of power system during because generation and demand must match momentarily. In the past, flexibility was achieved by supply side of the power grid, i.e., synchronous generation such as thermal power plants. However, increasing the penetration of renewable energy sources, with their uncertain characteristics together with reducing the share of thermal power plants in the supply side requires new sources of flexibility in the power grids [2]. As a result, efforts have been made to procure required energy flexibility from the demand side of power systems [3]. Demand-side flexibility can be used in different ways depending on the nature of the demand flexibility and the duration over which it can sustain a change in load [4]. For instance, it can be used for frequency regulating with an immediate impact on the system operation, or in congestion management and voltage regulation at the distribution electricity network to postpone the expansion plans [5]. While there is nothing to prohibit many residential appliances from providing flexibility, in reality, however, only a few of them are capable of providing it in a reliable and effective way. Heat pumps (HPs) coupled with either active or passive thermal energy storage are one of the most promising sources of flexibility from end-users [6]. Thermal inertia of buildings and thermal energy storage units together can help us to shift the operation of HPs in time. Moreover, power consumption level of HPs is typically high compared to other appliances, thus making them capable of providing a greater amount of flexibility when available.

The growing interest in exploiting the flexibility of HPs can be seen in the number of papers published on this topic in recent years. Schibuola et al. [7] investigated different heuristic price-based control strategies for an electric HP coupled with thermal energy storage and PV panels to minimize energy costs and self-consumption of locally produced electricity under a dynamic electricity tariff. Similarly, Rodriguez et al. in [8] analyzed the potential benefits of demand response strategies for HPs incentivized by day-ahead pricing signals. Yuan et al. [9] proposed a price-based method for controlling the water and space temperature of a swimming hall using district heating. A rule-based algorithm is used to exploit peak shaving and load shifting demand response programs, which led to 1.1% reduction in total energy cost and 3% increase in the average water temperature. The influence of electricity tariffs on energy flexibility in buildings and associated energy costs was investigated by Fizpatrick et al. [10]. The authors showed that real-time pricing is the most favourable tariff structure, capable of offering the greatest energy flexibility with lowest associated electricity costs. Baeten et al. [11] studied the impact of a large-scale deployment of actively controlled HPs and thermal energy storage on the power grid using a multi-objective predictive control (MPC) strategy. The optimal sizing strategy of domestic air-source HPs with thermal storage considering different electrical load shifting strategies in different dwellings was investigated by Marini et al. [12]. Their results showed that the amount of flexibility can change by consumption pattern, thermal energy storage volume and the electricity tariff.

Unlike the previous works which are mainly based on simulations, Müller et al. [13] presented the results from a large-scale trial of a demand response scheme involving a population of more than 300 residential buildings with HPs. Similarly, Sweetnam et al. [14] presented results of a trial of a control system aimed at optimising HP operation, within a time-varying electricity tariffs framework. In [15], Pèan et al. developed and experimentally tested different MPC strategies for space heating in a semi-virtual environment laboratory setup. The aim of the controller was to minimize either the delivered thermal energy to the building, the operational costs of the HP, or the CO_2 emissions related to HP operation. A rule-based control strategy for an air-source HP coupled with PV panels for heating applications was proposed by Bee et al. [16] in an Italian context with the purpose of enhancing the level of self-consumption. Fischer et al. [17] analyzed different operational strategies for capacity-controlled HPs connected to thermal storage in German multifamily houses to maximize energy performance and utilisation of on-site PV production, while minimizing energy costs. Leerbeck et al. [18] developed an optimal controller using model predictive control and external parameters such as weather and CO_2 emission forecasts, to minimize CO_2 emissions of buildings equipped with a HP unit.

Rominger et al. [19] experimentally investigated a new system architecture to provide frequency containment reserve through aggregation of heating, ventilation, and air conditioning systems. An industrial site containing workshop and office buildings, where the proposed architecture was installed and pre-qualified by the transmission system operators, was used as a case study. It has been shown that the system was capable of providing almost 300kW of frequency containment reserve. The technical and financial viability of the use of HPs to participate in the frequency restoration reserve market was investigated by Rodriguez et al. [20]. A simulation model was developed and validated using data from a household in a plus-energy neighborhood in southern Germany. Kim

4

et al. [21] analyzed the extent to which a direct load control strategy can unlock the energy flexibility potential of a commercial building equipped with a variable speed HP for frequency regulation. A coordinated control strategy of HP water heaters has been proposed by Mufaris et al. in [22] to minimize voltage violation and reverse power flow due to local PV generation in a residential distribution system in Japan. The results showed the effectiveness of the proposed coordinated control method in mitigating voltage violations without compromising end-user comfort, namely no shortage of domestic hot water during voltage control periods.

Our extensive literature review shows that we can categorize these papers in two main groups, 1) studies that focused on exploiting the implicit flexibility of HPs, i.e., [7]-[18], and 2) research works that developed algorithms to procure flexibility of HPs explicitly, i.e., [19]-[22]. In implicit flexibility procurement, the flexibility is obtained by offering time-varying electricity prices to the end-users. In explicit flexibility, however, end users' flexibility is offered to energy markets (e.g. through an aggregator) and a payment is received in return for the load variation offered and accepted in the market [23].

This paper proposes an approach to exploit the maximum explicit flexibility of HPs for participation in the power regulation market. Our focus is on using HPs in swimming pool heating systems (SPHSs), which is found to be an ideal flexibility resource in many studies [9] [24] [25] due to the high thermal storage capacity of the pools . Moreover, there are companies that provide large number of rental properties equipped with pools heated by HPs. For instance, NOVASOL manages more than 900 summerhouses with indoor pools in Denmark alone [26]. Making contracts with these companies gives the aggregators an access to significant flexibility of SPHSs that can be used to offer different services to the power grid. The main idea of the paper originates from the fact that it is not possible to utilize the flexibility of SPHSs throughout a day without any uncertainty because of their operational limits. This, in turn, increases the risk of bidding their flexibility capacity in the regulation market because the anticipated flexibility may not realise in real-time. To address this issue, we suggest tying the availability of SPHSs for flexibility provision to specific hours of a day, which is called a contract hour set (CHS). Each hour of a CHS is called a contract hour. The aggregator and end-user negotiate and agree on the service hours for the contract period. During each contract hour, the SPHSs are ready to respond to the requests issued by the aggregator. For instance, if the SPHS is supposed to provide downward reserve (more power consumption), it must remain off during the contract hours. Then, if the downward regulation reserve is needed in the power grids during the contract hour, the SPHS will be turned on and stays on until the end of the hour.

Since occurring power imbalance in the grid and its volume at each hour of the day is hard to predict, there is an uncertainty in utilizing the flexibility of SPHSs by the aggregator. This uncertainty must be considered in the proposed method. Moreover, parameters like building occupancy, electricity prices, weather condition, and initial state of system variables affect the feasibility of the plan; hence, should be included in the model.

The results of the proposed methodology provide a guideline for both aggregators and end-users before agreeing on a flexibility contract. This guideline gives a group of efficient CHSs in which a SPHS can provide maximum explicit flexibility for an aggregator without violating the users' comfort level above a certain threshold.

The main contributions of the paper are as follows:

1. Proposing a framework to procure the flexibility of SPHSs in specific hours of the day, without violating operational constraints and with no uncertainty in response to the flexibility request. The latter means the response to the flexibility request from the aggregator will always be positive in specific hours of the day; which guarantees a certain capacity for aggregator to bid in ancillary service markets, e.g., regulation market.

2. Introducing a stochastic mixed integer linear programming (SMILP) method for modeling the optimal operation of SPHSs considering the uncertainties in weather, electricity prices, initial state of the system variables, and using the available flexibility in each contract hour;

3. Proposing an analytical approach for obtaining a group of CHSs among all possible combinations of contract hours that maximizes the available flexibility while respecting the operational constraints of the system.

The rest of the paper is organized as follows. The problem definition and assumptions are presented in Section 2. In Section 3, different uncertainties in the system are introduced. The proposed approach for finding the most efficient CHSs is presented in Section 4. Simulation results are presented in Section 5. Finally, the paper is concluded in Section 6.

2. Problem assumptions and definition

As mentioned before, this paper focuses on SPHSs in summerhouses. These summerhouses are owned by a company and rented out on a daily/weekly basis. The swimming pools are indoor. However, we had only access to the swimming pool based on the agreement with the rental agency. Therefore, the control strategy is applied only to the SPHS. The main structure of the SPHS is presented in Fig. 1. The energy management system (EMS) receives price, weather and a summerhouse's booking status from data providers and also ambient and water temperature data from metering devices, and creates optimal control signals (ON or OFF status) for the operation of the SPHS in the next time intervals. The HP is equipped with a controller that determines ON/OFF status of the HP based on the deviation of water temperature from a set-point. So, to apply the control signal provided by the EMS to the HP, the temperature set-point will be adjusted accordingly. For instance, if the HP should be OFF (ON) in the next time interval, the
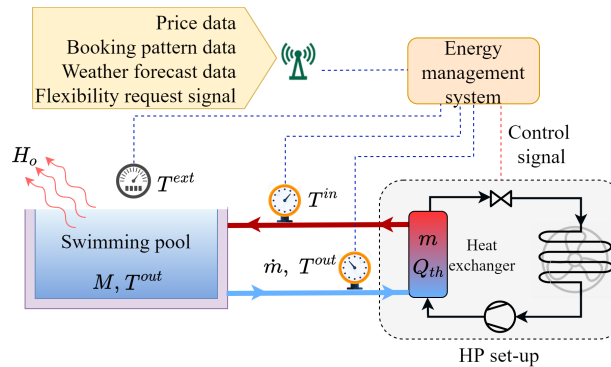

Figure 1: A typical structure of a SPHS in a summerhouse.

6

temperature set-point is changed to a lower (higher) temperature than the current pool water temperature. The EMS is ready at all times to receive a flexibility request from an aggregator to provide flexibility.

The best way to use the SPHSs' flexibility effectively is to aggregate a large number of them into a single flexibility source using a flexibility contract through an aggregator. Then, the aggregator can bid this flexibility in the regulation market. Since SPHSs' capability to provide flexibility is limited by operational constraints and the occupant comfort requirements, i.e., upper and lower limits of water temperature, their flexibility cannot be sustained for a long time. As a result, it is beneficial to end-users and aggregators to schedule flexibility of SPHSs for certain hours of a day through a CHS. The duration of a flexibility contract can be a day, week, month, season or year. Without loss of generality, however, the problem is discussed for a one month contract period in the rest of the paper.

Based on the flexibility contract, the SPHSs should be ready to provide flexibility for the aggregator during a specific CHS. Two parameters should be specified in the contract: 1) the type of flexibility i.e., upward or downward, that is supposed to be provided, and 2) agreed efficient CHSs for each possible occupation pattern of the summerhouse. During the operation period, before participating in the regulation market, the aggregator should be informed about the occupation of the summerhouses to choose the right CHS from the flexibility contract and calculate the available flexibility accurately.

Different CHSs are agreed by both parties for each occupation pattern because the water temperature limitations and consequently the ability to provide flexibility at each occupation pattern is different. It is assumed that the occupation status changes at 12:00 a.m. So, for each day, four main booking patterns can be defined. Water temperature limitations, and the ability to provide flexibility at each day depends on the occupation pattern of that day and the days before and after that. During the rented hours, water temperature limitations are more than other hours. Moreover, if the house is not rented for a long time, temperature limitations will be different from the case that it was unoccupied for only one day between two rented days. When the house is not rented for more than one day, temperature limitations are relieved as much as possible to reduce the use of SPHS. As a result, no flexibility services will be provided to the power grids until the beginning of the next rented day. However, when the house is not rented for only one day, there are still limitations on the water temperature to keep the swimming pool ready for the next day and flexibility services can also be provided for the grid. Considering the explanations above, possible occupation patterns and flexibility provision ability for each pattern is depicted in Fig. 2. No flexibility services are provided in occupation pattern (e) and the last 12 hours of occupation pattern (d). Therefore, the flexibility contract will be executed only for occupation patterns (a), (b), (c), (f), and the first 12 hours of occupation pattern (d).

It is useful for end-users as well as aggregators to have several options for each booking pattern as suitable CHSs to choose from. In this case, the aggregator can choose an optimal combination of CHSs from different contracts to maximize its profit by optimally bidding in the market. Therefore, the goal of the aggregator is to find a group of CHSs for each summerhouse that gives the parties a flexibility in choosing the suitable CHS. The main objective of this study is to propose a framework to find the most efficient CHSs at each occupation pattern for a SPHS. By an efficient CHS we mean a CHS with
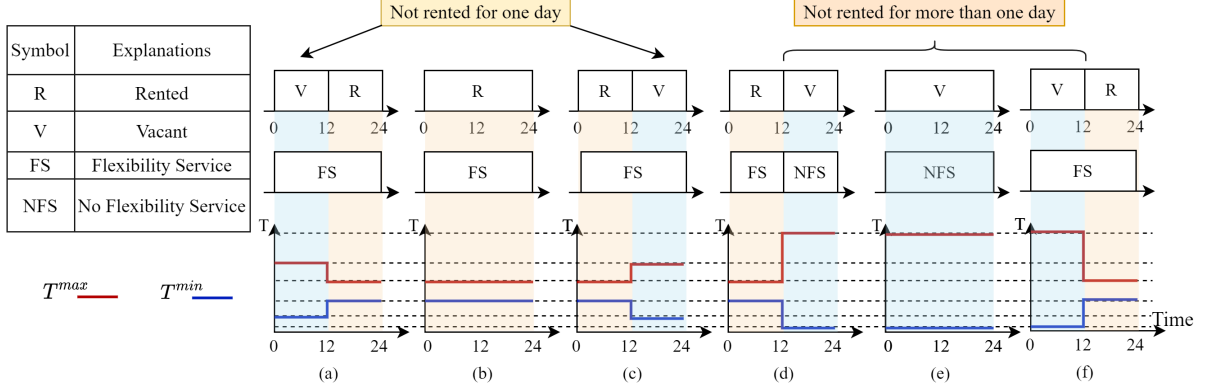
Figure 2: Possible occupation patterns, flexibility service availability, and related water temperature limitations for a typical summerhouse.

maximum number of contract hours that satisfies the end-user comfort constraints above a predefined threshold. This threshold represents the percentage of expected hours in different scenarios during which comfort constraints of users should be satisfied.

It should be noted that in addition to providing flexibility during CHSs (explicit flexibility), the operation of SPHS during all 24 hours of the day should be cost efficient (implicit flexibility). Therefore, feasibility of a CHS for the SPHS should be verified using an optimization problem that aims to minimize the total operation cost considering the flexibility contract. One of the main challenges regarding the flexibility contract modeling is uncertainty in exploiting SPHS flexibility for regulation power market. A comprehensive solution must take this uncertainty into account by solving a stochastic problem. Since at each booking pattern, one CHS is agreed for the whole contract period, the uncertainty in the ambient temperature, electricity prices, and initial state of system variables should also be included in the model for the scheduling horizon when the contract is for more than one day.

In this study, we focused on the problem at the building level, i.e., studying a single SPHS; thus we present an approach for finding a group of efficient CHSs for occupation patterns (a), (b), (c), (f), and the first 12 hours of booking pattern (d).

3. Introducing problem uncertainties

We categorized the different sources of uncertainties into two groups, 1) system uncertainties and 2) flexibility request uncertainties. Weather temperature, electricity price and a system's initial state are considered as the system uncertainties, while the uncertainties related to receiving a flexibility request from the aggregator in the next contract hours are called the flexibility request uncertainties.

3.1. System uncertainties

When the daily scheduling of the SPHS is performed, the electricity prices and weather temperature for the next 24 hours and initial water temperature of the swimming pool are known. However, in the case of multi-day contracts, these values are changing day by day. As a result, uncertainty scenarios should be produced to represent the variations in these parameters during the contract period.

Different methods such as using historic data or probabilistic forecasting approaches can

8

be used to produce these scenarios [27] [28]. In this paper, it is suggested to use historical data of the same interval of the contract period for creating electricity prices and weather temperature scenarios. However, probabilistic forecasting approaches can be used in real case implementations. Since the number of obtained scenarios of historical data is high, the backward scenario reduction method in [29] (briefly explained in Appendix A) is used to reduce the number of price and weather temperature scenarios to n_p and n_w, respectively. Each of these scenarios contains 24 electricity prices or temperature data for 24 hours of a day.

For initial water temperature uncertainty scenarios, if the historical data of the input and output water temperatures of the swimming pool are available, we can use it to produce these uncertainty scenarios. Otherwise, we can simulate the system for several days under different prices and ambient temperature to obtain water temperature values. Then, the temperature values at hour 00:00 of each day can be used for initial state scenario generation for the relevant booking pattern. Similar to price and weather uncertainty scenarios, using the backward scenario reduction method, the number of scenarios are reduced to n_l.

Merging the price, weather and initial state scenarios into one set of system uncertainty scenarios is preferred in order to reduce the complexity of the models in our paper. Each system uncertainty scenario includes three sets of values for 24 hour electricity prices, ambient temperature, and two values for initial input and output water temperatures of a swimming pool. To produce system uncertainty scenarios, all combinations of these three sets should be calculated, which equals $n_s = n_p \times n_w \times n_l$ that are recorded in the S set. The probability of each system uncertainty scenario is calculated by multiplying the probability of its related price, ambient temperature and initial state scenarios.

3.2. Flexibility request uncertainties

While the SPHS is ready to provide flexibility during contract hours, there is an uncertainty about utilizing this flexibility by the aggregator due to the uncertainty in the regulation power market. In this study, we assume that the EMS in the summerhouse considers these uncertainties and updates the operation schedule of the SPHS during the day based on the aggregator's actions, whether activating the flexibility or not. A scenario tree is used to model these uncertainties, as shown in Fig. 3, where it is assumed that the CHS is the set of hours $\{u, v, w\}$. If $t < u$, there is no contract hour and consequently, no flexibility request uncertainty in time intervals $t < u$. Hence, there will be a unique schedule for the SPHS, i.e., $u_{t,u}^i$ in time intervals $t < u$. For $u \leqslant t < v$, the optimal value of the HP's control variable depends on whether the flexibility in hour u is used by the aggregator, i.e., $s_u = 1$, or not, i.e., $s_u = 2$. Hence, the HP's control variable in time interval $u \leqslant t < v$ can be represented by $u_{t,s_u}^{i,uv}$. Similarly, the control variables in time intervals $v \leqslant t < w$ and $w \leqslant t$ are expressed by $u_{t,s_u,s_v}^{i,uv}$ and $u_{t,s_u,s_v,s_w}^{i,w}$, respectively.

4. The proposed approach for finding efficient CHSs

In this section, the process of finding a group of CHSs for a flexibility contract is presented in three main steps as follows:

1. **Step 1:** An optimization problem is formulated to obtain optimal scheduling of the SPHS considering the uncertainties in electricity prices, ambient temperature, initial state of system variables, and chance of flexibility being used by the aggregator.
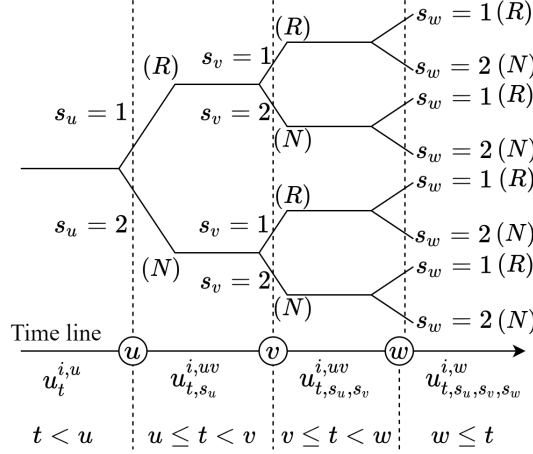
9

Figure 3: Scenario tree for modeling the uncertainty of requesting flexibility from the aggregator.

2. **Step 2:** A new metric is formulated to evaluate the effectiveness of each CHS in satisfying water temperature limitations using the results of the first step.

3. **Step 3:** Finally, an algorithm is suggested to find the group of most efficient CHSs using the recommended metric in the second step.

These steps are explained in detail in the following subsections.

4.1. Step 1: Optimal SPHS's operation formulation

In this section, the proposed formulation for determining the optimal daily operation of the SPHS is presented considering the system and flexibility request uncertainties. Therefore, a mathematical model representing the dynamics of the water temperature is needed. According to Fig. 1 and the proposed method by Zemtsov et al. in [30], these dynamics can be modeled by two differential equations. The first equation represents the power balance in the heat exchange and is formulated as below:

$$C_{in}\dot{T}_{t,s_a,s_b,...,s_z}^{in,i} = H_w(T_{t,s_a,s_b,...,s_z}^{out,i} - T_{t,s_a,s_b,...,s_z}^{in,i}) + Q_{th}u_{t,s_a,s_b,...,s_z}^i$$
$$\forall i \in S, s_a = 1,2,...,s_z = 1,2 \qquad (1)$$

where $C_{in} = m \times c_p$ and $H_w = \dot{m} \times c_p$ (see Fig. 1). The thermal power is calculated as $Q_{th} = COP \times P_n$, where COP represents the coefficient of performance and is assumed to be constant and P_n is the rated power of the HP. The second equation is the power balance in the pool and is presented below:

$$C_{out}\dot{T}_{t,s_a,s_b,...,s_z}^{out,i} = H_w(T_{t,s_a,s_b,...,s_z}^{in,i} - T_{t,s_a,s_b,...,s_z}^{out,i}) + H_o(T_t^{ext,i} - T_{t,s_a,s_b,...,s_z}^{out,i})$$
$$\forall i \in S, s_a = 1,2,...,s_z = 1,2 \qquad (2)$$

where $C_{out} = M \times c_p$ and H_o represents the overall heat transfer coefficient of the pool (see Fig. 1).

The optimization problem formulation is proposed for utilizing downward flexibility in which the HP is OFF at the contract hours and will be turned ON upon an aggregator's request. Conversely, if upward flexibility is needed, the HP must be ON at the contract

10

hours so that it can be turned OFF if the flexibility is requested. As far as the formulation is concerned, there is only one difference between the two flexibility formulations, which is the probability for activating flexibility by the aggregator. Therefore, the formulation is only presented for the downward flexibility procurement. The proposed formulation avoids infeasibility by leading to the results with lowest violations from water temperature limitations. Assuming the CHS is denoted by $\{a, b, c, ..., z\}$, the following formulation must be solved:

$$\min_{u^i} \quad \sum_{i \in S} \rho_i \sum_{s_a=1}^{2} \rho_{s_a}^a \sum_{s_b=1}^{2} \rho_{s_b}^b \times ... \times \sum_{s_z=1}^{2} \rho_{s_z}^z (\sum_{t \in N} C_t^i u_{t,s_a,s_b,...,s_z}^i \Delta t$$

$$+ \sum_{t \in N} \beta_t (v_{t,s_a,s_b,...,s_z}^i + w_{t,s_a,s_b,...,s_z}^i)) \quad (3)$$

$$\text{s.t.:} \quad T_{t,s_a,s_b,...,s_z}^{out,i} \geq T_t^{min} - v_{t,s_a,s_b,...,s_z}^i \qquad \forall i \in S, t \in N, s_a = 1, 2, ..., s_z = 1, 2 \quad (4)$$

$$T_{t,s_a,s_b,...,s_z}^{out,i} \leq T_t^{max} + v_{t,s_a,s_b,...,s_z}^i \qquad \forall i \in S, t \in N, s_a = 1, 2, ..., s_z = 1, 2 \quad (5)$$

$$T_{t,s_a,s_b,...,s_z}^{in,i} \geq T_t^{min} - w_{t,s_a,s_b,...,s_z}^i \qquad \forall i \in S, t \in N, s_a = 1, 2, ..., s_z = 1, 2 \quad (6)$$

$$T_{t,s_a,s_b,...,s_z}^{in,i} \leq T_t^{max} + w_{t,s_a,s_b,...,s_z}^i \qquad \forall i \in S, t \in N, s_a = 1, 2, ..., s_z = 1, 2 \quad (7)$$

$$u_{a,s_a}^i = \begin{cases} 0 & s_a = 1 \\ 1 & s_a = 2 \end{cases}, u_{b,s_a,s_b}^i = \begin{cases} 0 & s_b = 1 \\ 1 & s_b = 2 \end{cases}, ..., u_{z,s_a,s_b,...,s_z}^i = \begin{cases} 0 & s_z = 1 \\ 1 & s_z = 2 \end{cases}, \quad (8)$$

$Equations\ (1)\ and\ (2)$

The first term in the objective function (i.e., (3)) represents the total cost of electricity consumption by the SPHS. $u_{t,s_a,s_b,...,s_z}^i$ is the SPHS's operation decision variable, which is a binary variable. According to Fig. 3, we have:

$$u_{t,s_a,s_b,...,s_z}^i = \begin{pmatrix} u_t^{i,a} & t < a \\ u_{t,s_a}^{i,ab} & a \leqslant t < b \\ u_{t,s_a,s_b}^{i,bc} & b \leqslant t < c \\ ... & \\ u_{t,s_a,s_b,...,s_z}^{i,z} & z \leqslant t \end{pmatrix} \quad (9)$$

Please note that the optimization is solved for each CHS individually and the payment is made based on the capacity. Therefore, the revenue from providing flexibility is a constant term; hence is not considered in the objective function.

The second term in Eq. (3) refers to a penalty function that is added to the objective function to avoid infeasibility in results. Slack variables $v_{t,s_a,s_b,...,s_z}^i$ and $w_{t,s_a,s_b,...,s_z}^i$ in the penalty function represent the minimum violation of the swimming pool water temperature constraints that is needed to avoid infeasibility in the scheduling program. $v_{t,s_a,s_b,...,s_z}^i$ and $w_{t,s_a,s_b,...,s_z}^i$ are also defined as below:

$$v^i_{t,s_a,s_b,\dots,s_z} = \begin{pmatrix} v^{i,a}_t & t < a \\ v^{i,ab}_{t,s_a} & a \leqslant t < b \\ v^{i,bc}_{t,s_a,s_b} & b \leqslant t < c \\ \dots \\ w^{i,z}_{t,s_a,s_b,\dots,s_z} & z \leqslant t \end{pmatrix} \tag{10}$$

$$w^i_{t,s_a,s_b,\dots,s_z} = \begin{pmatrix} w^{i,a}_t & t < a \\ w^{i,ab}_{t,s_a} & a \leqslant t < b \\ w^{i,bc}_{t,s_a,s_b} & b \leqslant t < c \\ \dots \\ w^{i,z}_{t,s_a,s_b,\dots,s_z} & z \leqslant t \end{pmatrix} \tag{11}$$

β_t is a weighting coefficient that helps to prioritize violating comfort constraints in different hours. For instance, greater values of β_t means that the summerhouse is rented during those hours. This way, the temperature violations, if inevitable, occur during the summerhouse's vacant hours in an attempt to provide higher comfort for the occupants.

The constraints in Eqs.(4)-(7) represent the limits for input and output water temperature of the swimming pool. When the optimization problem is feasible, variables $v^i_{t,s_a,s_b,\dots,s_z}$ and $w^i_{t,s_a,s_b,\dots,s_z}$ are equal to zero and upper and lower bounds of the water temperature are limited to T^{max}_t and T^{min}_t, respectively. When a feasible solution cannot be reached, these upper and lower bounds are changed by $v^i_{t,s_a,s_b,\dots,s_z}$ and $w^i_{t,s_a,s_b,\dots,s_z}$ to keep the optimization problem feasible while finding a scheduling plan for the SPHS that leads to the lowest possible violation in the water temperature limits.

Equality constraints in Eq. (8) represent the uncertainty scenarios of flexibility request. This means that if the CHS include hour a, two scenarios can happen for the operation of HP in that hour, i.e., requesting (ON) or not requesting (OFF) flexibility. Equations (1) and (2) describe the dynamics of the system. In order to form a SMILP model, first, Eqs. (1) and (2) should be discretized, as in Eq. (12):

$$\underbrace{\begin{pmatrix} T^{in,i}_{t+1,s_a,s_b,\dots,s_z} \\ T^{out,i}_{t+1,s_a,s_b,\dots,s_z} \end{pmatrix}}_{\mathbf{T}_{t+1,s_a,s_b,\dots,s_z}} =$$

$$\underbrace{\begin{pmatrix} 1 - \frac{H_w \Delta t}{C_{in}} & \frac{H_w \Delta t}{C_{in}} \\ \frac{H_w \Delta t}{C_{out}} & 1 - \frac{H_w \Delta t}{C_{out}} - \frac{H_o \Delta t}{C_{out}} \end{pmatrix}}_{\mathbf{A}} \underbrace{\begin{pmatrix} T^{in,i}_{t,s_a,s_b,\dots,s_z} \\ T^{out,i}_{t,s_a,s_b,\dots,s_z} \end{pmatrix}}_{\mathbf{T}^i_{t,s_a,s_b,\dots,s_z}} + \underbrace{\begin{pmatrix} \frac{Q_n \Delta t}{C_{in}} \\ 0 \end{pmatrix}}_{\mathbf{B}} u^i_{t,s_a,s_b,\dots,s_z} + \underbrace{\begin{pmatrix} 0 \\ \frac{H_o \Delta t}{C_{out}} \end{pmatrix}}_{\mathbf{E}} T^{ext,i}_t \tag{12}$$

Then, by denoting the initial water temperature of the swimming pool in system uncertainty scenario i as $\mathbf{T}^i_t = \mathbf{T}^i_0$ and using Eq. (12), we can formulate the future states over the next N time intervals, as shown in Eqs. (13)-(15) [30]:

$$\mathbf{T}^i_{t+1,s_a,s_b,\dots,s_z} = \mathbf{A} \cdot \mathbf{T}^i_{t,s_a,s_b,\dots,s_z} + \mathbf{B} \cdot \mathbf{u}^i_{t,s_a,s_b,\dots,s_z} + \mathbf{E} \cdot \mathbf{T}^{ext,i}_t \tag{13}$$

$$\mathbf{T}^i_{t+2,s_a,s_b,\dots,s_z} = \mathbf{A} \cdot \mathbf{T}^i_{t+1,s_a,s_b,\dots,s_z} + \mathbf{B} \cdot \mathbf{u}^i_{t+1,s_a,s_b,\dots,s_z} + \mathbf{E} \cdot \mathbf{T}^{ext,i}_{t+1}$$

$$= \mathbf{A} \cdot \underbrace{\left[\mathbf{A} \cdot \mathbf{T}^i_{t,s_a,s_b,\dots,s_z} + \mathbf{B} \cdot \mathbf{u}^i_{t,s_a,s_b,\dots,s_z} + \mathbf{E} \cdot \mathbf{T}^{ext,i}_t \right]}_{\mathbf{T}^i_{t+1}} + \mathbf{B} \cdot \mathbf{u}^i_{t+1,s_a,s_b,\dots,s_z} + \mathbf{E} \cdot \mathbf{T}^{ext,i}_{t+1}$$

$$= \mathbf{A}^2 \cdot \mathbf{T}^i_{t,s_a,s_b,\dots,s_z} + \mathbf{AB} \cdot \mathbf{u}^i_{t,s_a,s_b,\dots,s_z} + \mathbf{B} \cdot \mathbf{u}^i_{t+1} + \mathbf{AE} \cdot \mathbf{T}^{ext,i}_{t,s_a,s_b,\dots,s_z} + \mathbf{E} \cdot \mathbf{T}^{ext,i}_{t+1} \quad (14)$$

$$\vdots$$

$$\mathbf{T}^i_{t+N,s_a,s_b,\dots,s_z} = \mathbf{A}^N \cdot \mathbf{T}^i_{t,s_a,s_b,\dots,s_z} + \sum_{j=1}^{N} \mathbf{A}^{N-j} \mathbf{B} \cdot \mathbf{u}^i_{t+j-1,s_a,s_b,\dots,s_z} + \sum_{j=1}^{N} \mathbf{A}^{N-j} \mathbf{E} \cdot \mathbf{T}^{ext,i}_{t+j-1} \quad (15)$$

Now, by defining the following parameters,

$$\mathbf{u}^i_{s_a,s_b,\dots,s_z} = \left[u^i_{1,s_a,s_b,\dots,s_z} \; u^i_{2,s_a,s_b,\dots,s_z} \; \dots \; u^i_{N,s_a,s_b,\dots,s_z} \right]^T \quad (16)$$

$$\mathbf{T}^{ext,i} = \left[T^{ext,i}_1 \; T^{ext,i}_2 \; \dots \; T^{ext,i}_N \right]^T \quad (17)$$

we can recast the above equations into the following linear equality constraints:

$$\mathbf{T}^i_{s_a,s_b,\dots,s_z} = \mathbf{F} \cdot \mathbf{T}^i_0 + \Psi \cdot \mathbf{u}^i_{s_a,s_b,\dots,s_z} + \Phi \cdot \mathbf{T}^{ext,i} \quad \forall m \in M, s_a = 1,2, s_b = 1,2,\dots, s_z = 1,2 \quad (18)$$

where,

$$\mathbf{T}^i_{s_a,s_b,\dots,s_z} = \begin{pmatrix} \begin{bmatrix} T^{in,i}_t \\ T^{out,i}_t \end{bmatrix} & t < a \\ \begin{bmatrix} T^{in,i}_{t,s_a} \\ T^{out,i}_{t,s_a} \end{bmatrix} & a \leqslant t < b \\ \begin{bmatrix} T^{in,i}_{t,s_a,s_b} \\ T^{out,i}_{t,s_a,s_b} \end{bmatrix} & b \leqslant t < c \\ \vdots \\ \begin{bmatrix} T^{in,i}_{t,s_a,s_b,\dots,s_z} \\ T^{out,i}_{t,s_a,s_b,\dots,s_z} \end{bmatrix} & z \leqslant t \end{pmatrix} \quad (19)$$

$$\mathbf{F} = \begin{pmatrix} \mathbf{A} \\ \mathbf{A}^2 \\ \mathbf{A}^3 \\ \vdots \\ \mathbf{A}^N \end{pmatrix} \quad (20)$$

$$\Psi = \begin{pmatrix} \mathbf{B} & \mathbf{0} & \mathbf{0} & \dots & \mathbf{0} \\ \mathbf{AB} & \mathbf{B} & \mathbf{0} & \dots & \mathbf{0} \\ \mathbf{A}^2\mathbf{B} & \mathbf{AB} & \mathbf{B} & \dots & \mathbf{0} \\ \vdots & \vdots & \vdots & & \vdots \\ \mathbf{A}^{N-1}\mathbf{B} & \mathbf{A}^{N-2}\mathbf{B} & \mathbf{A}^{N-3}\mathbf{B} & \dots & \mathbf{B} \end{pmatrix} \quad (21)$$

$$\Phi = \begin{pmatrix} \mathbf{E} & \mathbf{0} & \mathbf{0} & \dots & \mathbf{0} \\ \mathbf{AE} & \mathbf{E} & \mathbf{0} & \dots & \mathbf{0} \\ \mathbf{A^2E} & \mathbf{AE} & \mathbf{E} & \dots & \mathbf{0} \\ \vdots & \vdots & \vdots & & \vdots \\ \mathbf{A^{N-1}E} & \mathbf{A^{N-2}E} & \mathbf{A^{N-3}E} & \dots & \mathbf{E} \end{pmatrix} \tag{22}$$

T_{ext}^i is the weather temperature vector that includes hourly temperature values of a day under uncertainty scenario i.

Now, replacing the system dynamic equations (1) and (2) by the linear equation (18), the optimization problem in Eqs. (3)-(8) and (18) forms a SMILP problem that can be solved by CPLEX solver in GAMS.

4.2. Step 2: Introducing the evaluation index for CHSs

The effectiveness of each CHS as a successful contract plan is measured using a metric, which is specified by K^0. The metric is defined as the percentage of the time intervals among all hours in all scenarios, i.e, $N \times n_s$, that the water temperature limitations are satisfied. Since $v_{t,s_a,s_b,\dots,s_z}^i$ and $w_{t,s_a,s_b,\dots,s_z}^i$ represent the violations of the water temperature limits in different hours and scenarios, we use these variables to calculate the metric for each CHS as below:

$$I_{t,s_a,s_b,\dots,s_z}^{1,i} = \begin{cases} 0 & v_{t,s_a,s_b,\dots,s_z}^i > 0 \\ 1 & otherwise \end{cases} \tag{23}$$

$$I_{t,s_a,s_b,\dots,s_z}^{2,i} = \begin{cases} 0 & w_{t,s_a,s_b,\dots,s_z}^i > 0 \\ 1 & otherwise \end{cases}, \tag{24}$$

$$K^0 = \sum_{m=1}^{n_s} \rho_i \sum_{s_a=1}^{2} \rho_{s_a}^a \sum_{s_b=1}^{2} \rho_{s_b}^b \times \dots \times \sum_{s_z=1}^{2} \rho_{s_z}^z \sum_{t=1}^{N} \left(\frac{I_{t,s_a,s_b,\dots,s_z}^{1,i} + I_{t,s_a,s_b,\dots,s_z}^{2,i}}{N \times n_s} \right) \times 100 \tag{25}$$

4.3. Step 3: Determining the group of most efficient CHSs

In this section, the proposed method for obtaining the group of efficient CHSs is presented for occupation patterns (a), (b), (c), (f), and the first 12 hours of occupation pattern (d) (as shown in Fig. 2). We can classify these patterns into two main types: 1) patterns (a), (c), and (f) in Fig. 2, which include both rented and vacant statuses and are called ACF occupation class, and 2) booking pattern (b) and the first 12 hours of the booking pattern (d) that include only rented status and are called the BD occupation class. A generic approach is proposed to find the group of most efficient CHSs for both occupation classes.

Trying all possible combinations, or using meta-heuristic optimization algorithms that are based on iterative methods is not efficient because the process of computing evaluation metrics for each CHS can be time consuming. Therefore, an analytical method is proposed to find the efficient CHSs in this study. Moreover, to reduce the computational burden, a standard format is defined to describe CHSs mathematically. Many formats can be defined for CHSs, however, our goal is to choose the formats that are easy to understand for both aggregators and end-users and efficient in covering a wide range of combination of hours as much as possible.

We define the contract hours sequences as $C_{X1,X2}^{|A1|,|A2|}(h)$, which includes two subsets $A1$ and $A2$. The symbol $|.|$ shows a set cardinality. The subset $A2$ has $|A2|$ contract hours
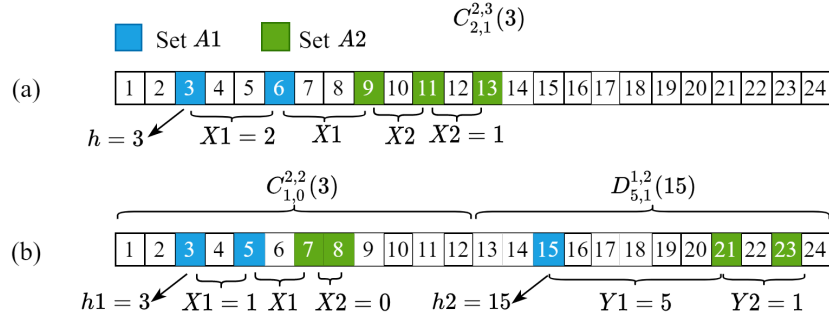
Figure 4: Illustrative examples of CHSs in occupation class BD with set $\{C_{X1,X2}^{|A1|,|A2|}(h)\}$ and b) occupation class ACF with set $\{C_{X1,X2}^{|A1|,|A2|}(h1), D_{Y1,Y2}^{|B1|,|B2|}(h2)\}$.

and comes right after subset $A1$ that also consists of $|A1|$ contract hours. The number of hours between each two contract hours in subset $|A1|$ ($|A2|$) is $X1$ ($X2$) hours. h represents the starting hour of the contract sequence. An illustrative example of this contract hours sequences is depicted in Fig. 4a.

A block-diagram of the proposed method for finding efficient CHSs is presented in Fig. 5 and explained below:

1. The first step is to determine the maximum number of contract hours for efficient CHSs. To that end, we use the fact that for the same number of contract hours, consecutive-hour CHSs (CHCHSs) can give a lower bound to the effectiveness of all combinations of CHSs with the same number of contract hours. This is true because the ability of an EMS in CHCHSs for correcting the deviations enforced by flexibility utilization is less than other combinations. CHCHSs can be defined by sets $\{C_{0,0}^{Z,0}(h)\}$, where Z is the number of contract hours. Since the efficiency of a CHCHS increases by converting it into a non-CHCHS, we suggest that the maximum number of contract hours at each booking pattern, i.e., $\bar{Z}$, be equal to the minimum number of contract hours in which for all combinations of CHCHSs (i.e., all possible values of h), K^0 values are less than a predetermined threshold. By turning $\bar{Z}$-hour CHCHSs into $\bar{Z}$-hour non-CHCHSs (increasing their efficiencies) in the next steps, efficient CHSs will be determined.

2. For each occupation pattern in the class BD, all possible non-CHCHSs in the form of $\{C_{X1,X2}^{|A1|,|A2|}(h) \mid \bar{Z} = |A1| + |A2|\}$ are created, the value of K^0 index for each CHS is calculated using Eq. (25), and the CHSs with K^0 index greater than the threshold are identified as efficient CHSs.

3. For ACF class, since there are both rented and vacant statuses in the occupation pattern, the standard CHS is defined as in set $\{C_{X1,X2}^{|A1|,|A2|}(h1), D_{Y1,Y2}^{|B1|,|B2|}(h2)\} \mid \bar{Z} = |A1| + |A2| + |B1| + |B2|$. Subset $A = C_{X1,X2}^{|A1|,|A2|}(h1)$ is used to describe the contract hours when the house is vacant, while subset $B = D_{Y1,Y2}^{|B1|,|B2|}(h2)$ describes the contract hours when the house is rented. An example of these CHSs is depicted in Fig. 4b. Efficient CHSs for occupation patterns in class ACF are obtained as follows:
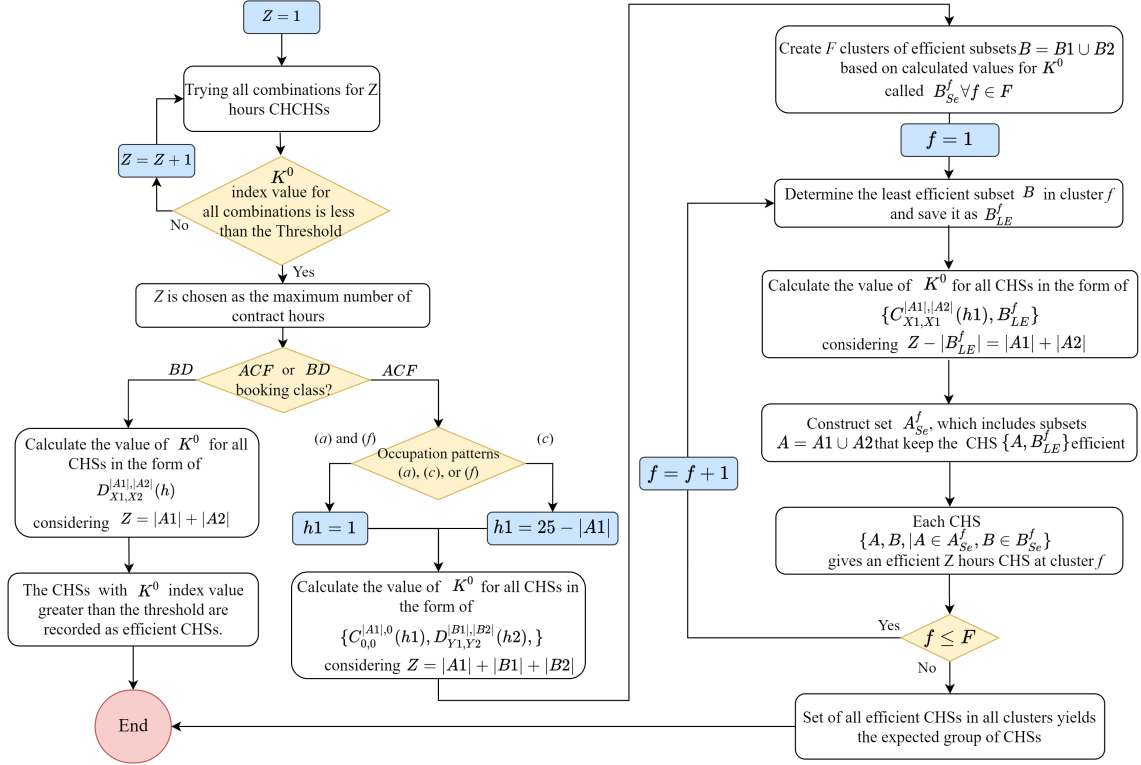
15

Figure 5: Process of determining the group of efficient CHSs.

- First, we find the most efficient subsets B by trying all their combinations while the rest of the contract hours in subset A are constant. Since our focus is on subset B in this step, the contract hours in subset A are defined in such a way that the impact of uncertainty caused by these contract hours on K^0 metric is minimized. Since temperature violations mainly occur during rental hours, subsets A are defined as CHCHSs in $C_{0,0}^{|A1|,0}(h1)$ format, where $h1 = 1$ for occupation patterns (a) and (f) and $h1 = 25 - |A1|$ for occupation pattern (c). Choosing these values for $h1$ maximizes the timespan between contract hours in subsets A and rental hours; hence minimizes their impacts on K^0 values. So, all possible combinations of CHSs in the forms of $\{C_{0,0}^{|A1|,0}(1), D_{Y1,Y2}^{|B1|,|B2|}(h2) \mid \bar{Z} = |A1| + |B1| + |B2|\}$ for occupation patterns (a) and (f) and $\{C_{0,0}^{|A1|,0}(25 - |A1|), D_{Y1,Y2}^{|B1|,|B2|}(h2) \mid \bar{Z} = |A1| + |B1| + |B2|\}$ for occupation patterns (c) are created and their related K^0 indices are calculated.

- Subsets B with K^0 greater than the threshold are identified and classified under F clusters. In each cluster, a) K^0 values should be in the same range and b) the number of contract hours in the subset B of CHSs should be the same. Determining the number of clusters and the range of K^0 values at each cluster depends on the occupation pattern and the defined threshold, and is performed after obtaining the efficient subsets B. The set of all subsets B in cluster f is called B_{Se}^f. The subset B of the least-efficient CHS in each cluster f is defined as B_{LE}^f.

- Since B_{LE}^f has the lowest efficiency among other subsets B in cluster f, if its

union with a subset $\{A \mid |A| = |\bar{Z}| - |B_{LE}^f|\}$ leads to an efficient CHS, the union of other subsets B in cluster f with this subset A will also lead to efficient CHSs. So, for each cluster f, all combinations in the form of $\{C_{X1,X2}^{|A1|,|A2|}(h), B_{LE}^f\}$ are investigated and their related K^0 indices are calculated. Subsets A, whose union with B_{LE}^f leads to efficient CHSs, are identified and recorded in a set called A_{Se}^f.

- At each cluster, the union of each subset $A \in A_{Se}^f$ and each subset $B \in B_{Se}^f$ gives an efficient CHS.

5. Numerical results

A summerhouse located in Denmark is chosen as the case study in this paper. Without loss of generality, September is chosen as the contract period. We define $n_p = n_w = n_i = 5$. In order to create price and weather uncertainty scenarios, day-ahead market prices and weather data from September 2020 are collected and then reduced to five scenarios as shown in Fig. 6. To create initial water temperature scenarios, 1000 scenarios including different prices, weather conditions, booking patterns, and initial states are generated for two consecutive days. Then, the SPHS scheduling result for each scenario is obtained using the proposed optimization problem in Section 4.1 after eliminating the uncertainty of flexibility request in the formulation. The values of input and output water temperature of the swimming pool at hour 00:00 of the second day is used as the initial input and output water temperature scenarios. These scenarios are reduced to five main scenarios using the backward scenario reduction method, as shown in Table 1. The probabilities of each price, weather and initial water temperature scenario are reported in Table 2. Considering different combinations of prices, weather and initial water temperature scenarios, 125 system uncertainty scenarios, i.e., $n_s = 125$, are obtained.

Lower and upper bounds of swimming pool water temperature during rented hours are $27\,^oC$s and $29\,^oC$s, respectively, while they change to $25\,^oC$s and $31\,^oC$s, respectively,
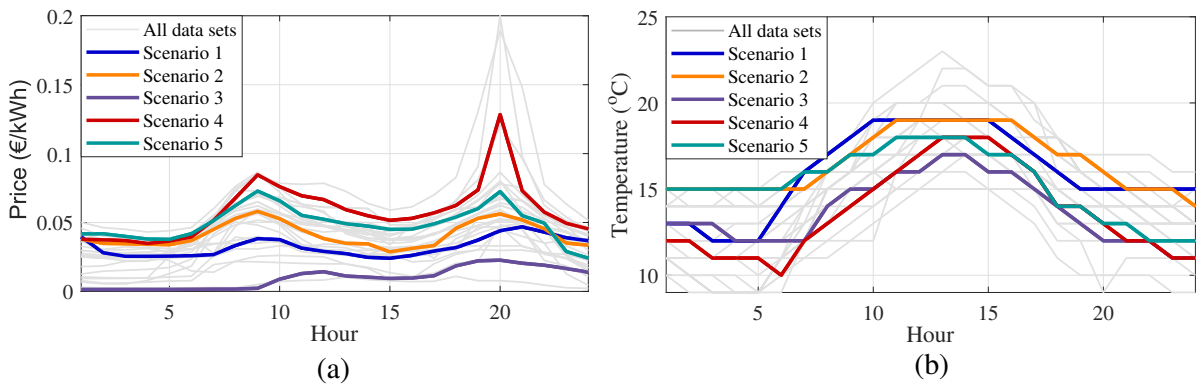

Figure 6: System uncertainty scenarios a) electricity prices, and b) ambient temperature.

Table 1: Uncertainty scenarios for initial water temperature of the swimming pool

Scenario Number	1	2	3	4	5
T_{in}^0	28.8	28	26.8	26.7	25.6
T_{out}^0	28.7	26.5	26.7	25.5	25.5

17

Table 2: Probability of each price, weather and initial water temperature scenario.

Scenario Number	1	2	3	4	5
Price	0.20	0.23	0.14	0.13	0.30
Weather temperature	0.17	0.20	0.16	0.30	0.17
Initial water temperature	0.24	0.02	0.58	0.04	0.12

Table 3: SPHS parameters for the simulation study.

C_{out} $(kWh/^oCs)$	C_{in} $(kWh/^oCs)$	H_{on} $(^oCs/kW)$	H_w $(^oCs/kW)$	Q_n (kW)	Δt (h)
80	10	0.5	15	30	1

during non-rented hours. Probability of procuring flexibility by the aggregator is assumed to be 0.5, i.e., $\rho_{s_a}^a = \rho_{s_b}^b = \cdots = \rho_{s_z}^z = 0.5$. In this case, the formulation and simulation results would be the same for both upward and downward regulation. Parameter β_t is equal to 2×10^3 and 10^3 during rented and non-rented hours, respectively. Comfort level threshold is assumed to be 98%, which means that maximum acceptable violation from the water temperature limits is 2% of the all time intervals during the contract periods. The SPHS parameters are defined in Table 3 [30]. The simulation results for occupation pattern (a) of Fig. 2 are discussed thoroughly. The results from other booking patterns are discussed briefly to avoid duplication and extra pages.

5.1. Investigating the impacts of different CHSs on the swimming pool water temperature variations

To illustrate how choosing a CHS with specific contract hours can affect the feasibility of SPHS's operation, the simulation results of swimming pool water temperature variations for two cases are compared in Fig. 7. In the first case, the CHS is chosen as $\{5, 6, 7\}$, where no violation of the water temperature limits has occurred, as shown in Fig. 7a. However, in the second case where CHS is $\{15, 16, 17\}$, water temperature limitations are violated in some hours and flexibility request scenarios, as depicted in Fig. 7b. Therefore, CHS of $\{5, 6, 7\}$ is more efficient than CHS of $\{15, 16, 17\}$ in this particular case.
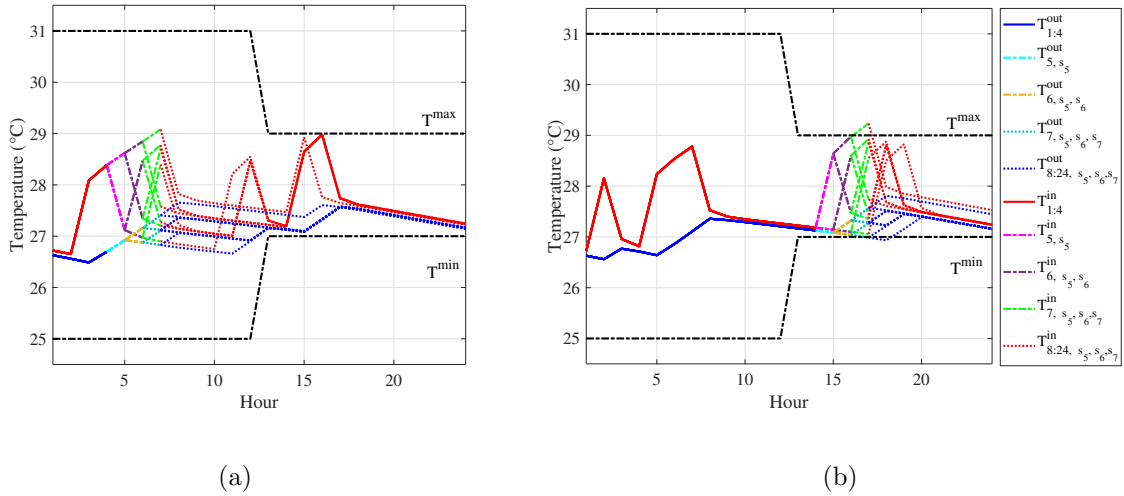

(a) (b)

Figure 7: Swimming pool water temperature variations in different flexibility scenarios and a specific system uncertainty scenario for the CHS a) $\{5, 6, 7\}$ and b) $\{15, 16, 17\}$.

18

5.2. Obtaining the group of efficient CHSs for occupation pattern (a)

In this subsection, the proposed algorithm from Section 4.3 and Fig. 5 is used to find the group of most efficient CHSs for occupation pattern (a) in Fig. 2.

5.2.1. Determining maximum number of contract hours

The first step is to find the maximum number of contract hours. To this end, values of evaluating index K^0 for all combinations of CHCHSs with 1 to 7 contract hours are calculated and presented in Fig. 8. Each point (h, k) on each curve in Fig. 8 represents a CHCHS whose first contract hour is h, and whose related index value is k. According to Fig. 8, we can conclude that:

- CHCHSs with equal or less than three contract hours satisfy the comfort level threshold.

- For CHCHSs with equal or less than four contract hours during non-rented times, violations of water temperature limitations are almost zero.

- All combinations of CHCHSs with $Z \geq 7$ do not satisfy the required threshold. According to the explanations in Section 4.3, a maximum of 7-hour contract duration is selected for efficient CHS, i.e., $\bar{Z} = 7$.
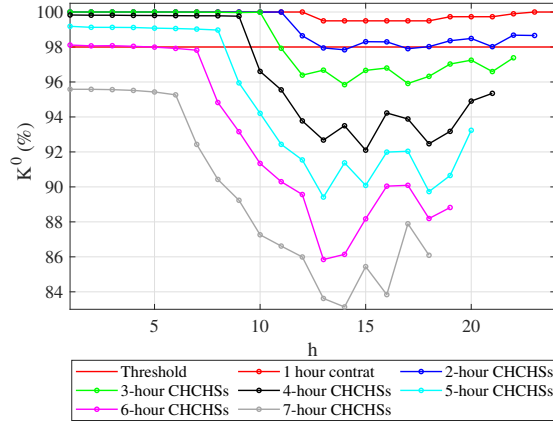

Figure 8: Values of evaluation index K^0 for 1 to 7 consecutive hour CHSs in occupation pattern (a).

5.2.2. Obtaining efficient subsets B

In this step, each 7-hour CHS is divided into two subsets A and B. According to section 4.3, contract hours in subset A should start from hour 1 and continue for several hours, i.e., $A = \{C_{0,0}^{|A|,0}(1) \mid |A| \leq \bar{Z}\}$. Subset B represents the contract hours of the CHS when a house is rented, i.e., $k > 12$, which is defined in the standard format of $B = \{C_{Y1,Y2}^{|B1|,|B2|}(h2)\}$, where $\bar{Z} - |A| = |B1| + |B2| = |B|$, and $h2 \geq 13$. Choosing the above-mentioned format for subset A minimizes the impact of the uncertainty caused by this subset on calculation of K^0; hence, the value of K^0 mostly depends on the structure

19

of subset B. By trying all possible combinations of subsets B, i.e., all possible values of $|B1|$, $|B2|$, $Y1$, $Y2$ and $h2$, and calculating K^0 index values, we can identify efficient subsets B that give efficient CHSs.

The simulation results show that:

- All subsets B with $|B| \leq 1$ or $|B| \geq 4$ do not lead to efficient subsets.

- All subsets B with $Y1 \leq 1$ or $Y2 \leq 1$ are inefficient.

- There are a few subsets with $|B| = 2, 3$ and $Y1 \geq 2$ and $Y2 \geq 2$ that give efficient CHSs, as shown in Fig. 9. In general, when $|B| = 2$, subsets are efficient for $h2 \geq 19$, while subsets are efficient for $h2 \geq 15$ when $|B| = 3$.

- As shown in Fig. 9, efficient subsets cover almost all the rented period except for hour 13. Therefore, the aggregator can provide flexibility at all hours by choosing different subsets B of CHSs for different contracted summerhouses.
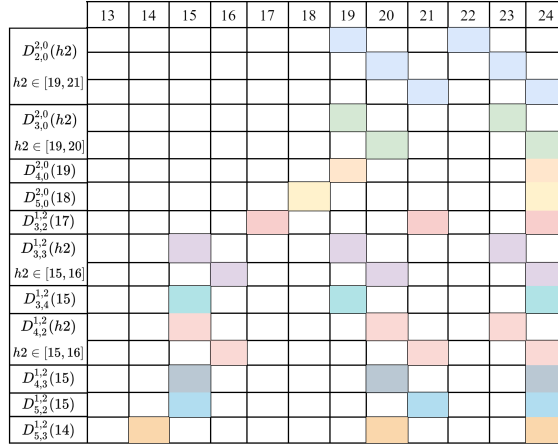

Figure 9: Illustrative representation of efficient subset B.

5.2.3. Clustering efficient subsets B and determining B_{LE}^f for each cluster

The next step in the algorithm proposed in Section 4.3 is clustering the efficient subsets B. As mentioned in Section 4.3, at each cluster, K^0 values should be in the same range, and the number of contract hours in the subset B should be the same. According to the results of Section 5.2.2, four clusters are defined, as shown in Fig. 10. At each cluster $f \in F$, all obtained efficient subsets B are recorded in B_{Se}^f.

The next step is to determine the least-efficient subset B at each cluster f, i.e., B_{LE}^f. These are the subsets with lowest K^0 index value of subset B in each cluster, which are presented in Table 4.

Table 4: Least-efficient subsets B in each cluster.

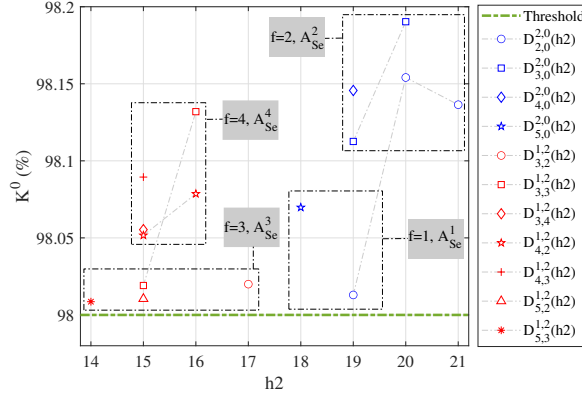| Cluster (f)	1	2	3	4
B_{LE}^f	$D_{2,0}^{2,0}(19)$	$D_{3,0}^{2,0}(19)$	$D_{5,3}^{1,2}(14)$	$D_{4,2}^{1,2}(15)$

Figure 10: Illustrative representation of efficient subsets B and the resultant clusters.

5.2.4. Obtaining efficient subsets A for B_{LE}^f in each cluster

Efficient subsets A in each cluster are the subsets whose union with subsets B at the same cluster leads to efficient CHSs. To find these efficient subsets A in each cluster, all combinations of CHSs in $\{A, B_{LE}^f\}$ format, where $A = \{C_{X1,X2}^{|A1|,|A2|}(h1) \mid Z - |B_{LE}^f| = |A1| + |A2|,\ 1 \leq h1 \leq 12\}$ are examined. The subsets A leading to K^0 greater than the threshold are chosen as efficient subsets A and recorded in the set $A_S^f e$. Simulation results show that in each cluster, there can be many efficient subsets A. To avoid complexity in presentation and provide an easy guideline for finding efficient subsets A, we suggest using an index to identify them in an easier way. The average of contract hours numbers (ACHN) at each subset A is used as an index to identify these subsets. In this case, a maximum ACHN can be defined for each cluster f that all subsets A with ACHNs smaller than this maximum value be efficient. The distribution of ACHNs of all combinations of subsets A at all clusters is presented in Fig. 11. Reviewing the simulation results shows the overlapping area of efficient and inefficient CHSs is large, highlighted in Fig. 11a on the left, which makes it difficult to distinguish between the ACHN intervals of efficient and inefficient subsets. To overcome this issue, subsets A in the overlapping area were studied, where we noticed that most of subsets A are the ones that include hour 12 as the contract hour. So, the simulations are repeated after removing these subsets A. In the new simulation results, it can be seen that the overlapping area decreases significantly, highlighted in Fig. 11a on the right. Now, we define the maximum acceptable value for ACHN of efficient subsets A at each cluster f, i.e., $ACHN_f^{max}$, as the average ACHN of efficient and inefficient subsets A in the overlapping area. Using this definition, $ACHN_f^{max}$ in clusters 1, 2, 3, and 4 are equal to 5.9, 7.53, 5.25, and 6.96, respectively. Then, we can define sets $A_{Se}^f = \{A \mid ACHN(A) \leq ACHN_f^{max}\ and\ 12 \notin \{A\}\}$. Although some inefficient ACHNs might be identified as efficient ACHNs in this case, they are rare and their efficiencies are very close to predetermined threshold. It should be noted that while most subsets A with contract hour 12 are inefficient, there are a few efficient subsets A in cluster 2 with contract hour 12 in the form of $C_{0,\{5,6,7\}}^{3,2}(12)$, $C_{1,4}^{3,2}(12)$ and $C_{0,2}^{2,3}(12)$.

Finally, efficient CHSs are obtained as $\{\{A, B\} \mid A \in A_{Se}^f,\ B \in B_{Se}^f,\ \forall f \in F\}$.

Based on the simulation results in Sections 5.2.1-5.2.4, it can be said that efficient CHSs for occupation pattern (a) of the summerhouse should have the following properties:

- The maximum number of contract hours for achieving the comfort level threshold
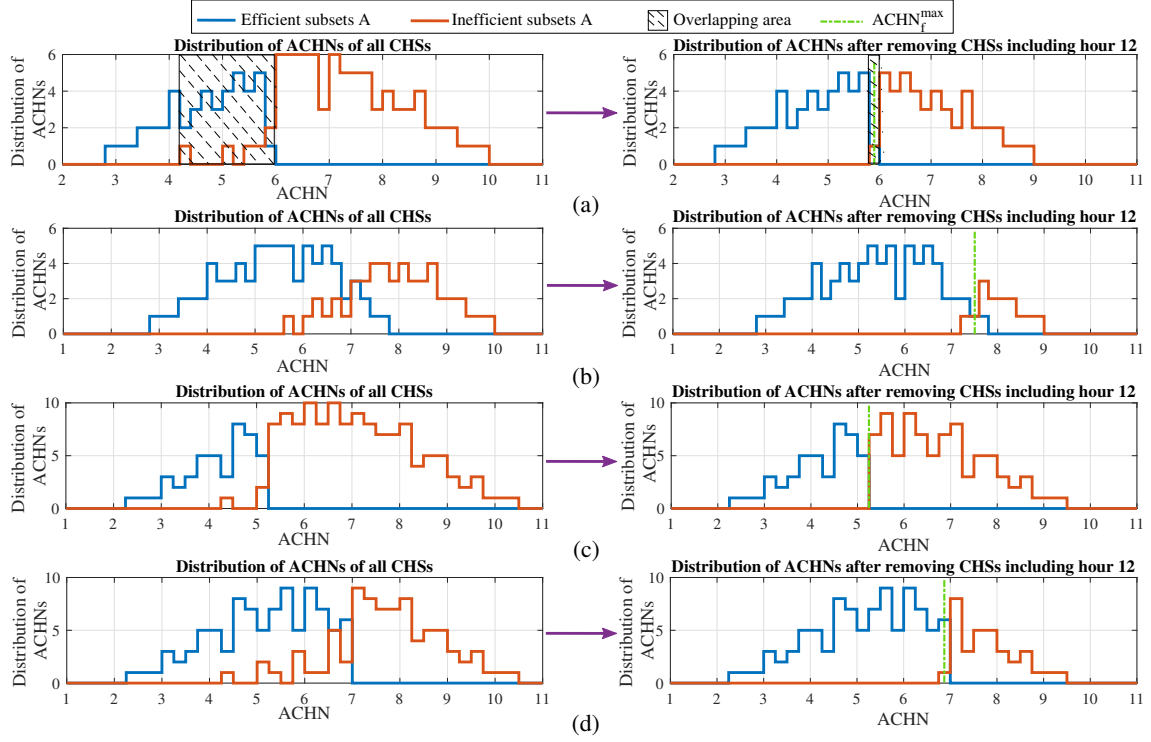
21

Figure 11: Distribution of ACHNs with and without CHSs with flexibility commitment at hour 12 in clusters a) 1, b) 2, c) 3, and d) 4.

98% is 7 hours.

- The contract hours during rented hours are recommended in $\{D_{Y1,0}^{2,0}(h2) \mid Y1 \geq 2,\ h2 \geq 19\}$ or $\{D_{Y1,Y2}^{1,2}(h2) \mid Y1 \geq 3,\ Y2 \geq 2,\ h2 \geq 15\}$ format.

- Most recommended subsets A of efficient CHSs are the ones that do not include hour 12 as a contract hour and their ACHN value are less than $ACHN_f^{max}\ \forall f \in F$ given in Fig. 11.

5.3. Evaluating the proposed method for choosing the maximum number of contract hours

In Section 4.3, a method was suggested to find the maximum number of contract hours. In this section, the effectiveness of this method is evaluated. To this end, the proposed approach is repeated for the case that the number of contract hours is eight. Fig. 12 illustrates some of the most efficient 8-hour CHSs. It can be seen that none of the 8-hour CHSs can reach efficiencies greater than 97%. If we want to use these types of CHS, we have to accept the risk of a higher rate of violation of the water temperature limits.

5.4. Obtaining the maximum number of contract hours for other occupation patterns

The same approach, as discussed in Section 5.2 for occupation pattern (a), can be employed to find the group of efficient CHSs in other occupation patterns. Here, we only present the results of the maximum number of contract hours. Following the method proposed in Section 4.3, the maximum number of contract hours, i.e., $\bar{Z}$, for each occupation pattern is reported in Table 5.
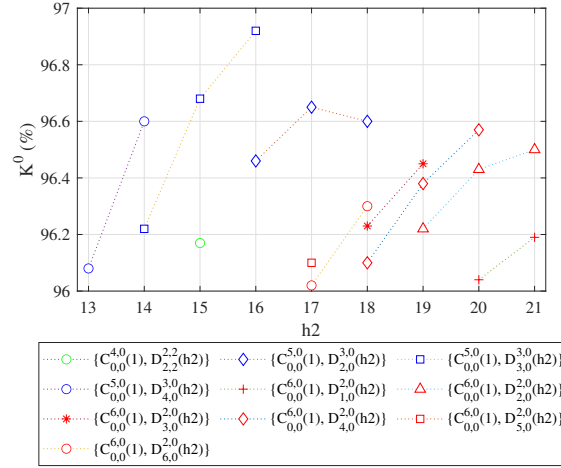
Figure 12: Most efficient 8-hour CHSs.

As shown in Table 5, in occupation patterns (b) and (d), the opportunity to provide flexibility decreases because the summerhouse is rented during the flexibility service provision hours and water temperature constraints are tight. As a result, the maximum number of contract hours would be 3 and 2 hours, respectively. The difference between occupation patterns (a) and (f) is in the water temperature limitations when the house is vacant. Although the temperature limitations are relaxed in occupation pattern (f), the maximum number of contract hours is fewer than the ones in occupation pattern (a). This happens because in occupation pattern (f), the SPHS is OFF in previous days, hence the initial water temperature is lower than other patterns. Therefore, the SPHS should be ON for a longer period of time to reach the desired temperature at 12 a.m., which leads to less flexibility in the SPHS operation. Occupation pattern (c) gives the highest number for contract hours among all occupation patterns. This is due to the fact that the house is not rented for 24 hours after hour 12 a.m., which gives the highest flexibility in operation in the last 12 hours of the day.

Table 5: Maximum number of contract hours for different occupation patterns.

	Occupation class ACF			Occupation class BD	
	a	c	f	b	d
Z	7	13	4	3	2

5.5. Cost-benefit analysis of flexibility contracts

The main driver for end-users to become involved in flexibility contracts is financial. However, involving in other power grids services deviates the operation of SPHS from its optimal operation point and increases the costs. In this section, the additional cost of providing flexibility services is investigated. To estimate the cost, 10 efficient CHSs with the maximum number of contract hours, as shown in Table 5, are generated for each occupation pattern. Then, average optimal operation cost of each occupation pattern is calculated and subtracted from the baseline operation cost, i.e., when there is no flexibility contract. The results are divided by the number of contract hours to obtain the cost incurred to the summerhouse per each contract hour in each booking pattern. Simulation
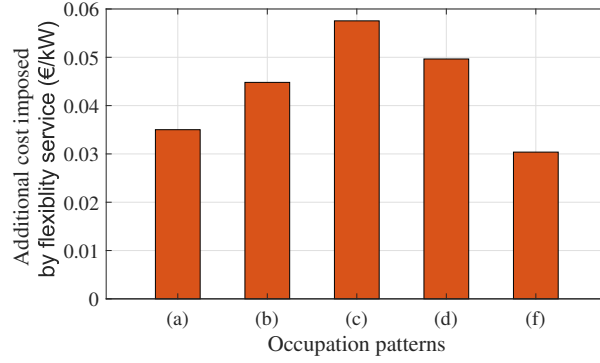
Figure 13: Expected cost of providing flexibility service in each contract hour for all occupation patterns.

results are presented in Fig. 13. It can be seen that the cost per kW of flexibility service in each pattern is different, which is due to differences in the maximum number of contract hours in each pattern and the hours of the day i.e., on-peak, mid-peak or off-peak, in which flexibility is requested. For instance, in occupation patterns (a) and (f), most of the contract hours occur during off-peak and mid-peak hours, which leads to decrease in their costs in case of utilizing their flexibility by the aggregator. However, most contract hours in occupation pattern (c) are selected during the mid-peak and on-peak hours, which increase the operation cost of the SPHS compared to other cases. This cost should be the minimum payment to the summerhouse owner to encourage them to provide flexibility services.

6. Conclusion

This paper proposes a methodology to procure maximum explicit flexibility of a swimming pool heating system without uncertainty in response to the flexibility request. To this end, a group of contract hour sets is obtained in which the heating system is ready to provide flexibility to an aggregator. The aggregator and end-user can agree on one specific contract hour set among all sets to provide flexibility during a contract period. In order to find these contract hour sets, first, a SMILP formulation is proposed to find the optimal daily scheduling of the swimming pool heating system considering operational constraints, uncertainty in price, weather and initial state of the system during the contract period, and uncertainty in utilizing the flexibility for a specific contract hour set. Then, an evaluation metric is formulated to measure the efficiency of a set in satisfying users' comfort constraints using the results of the first step. Finally, an algorithm is proposed to find the group of efficient contract hour sets with the maximum number of contract hours using the proposed evaluation metric in the second step.

The proposed method was applied to a summerhouse equipped with a indoor swimming pool heating system. Among all possible booking patterns, five booking patterns in which the heat pump can provide flexibility was chosen and maximum number of contract hours for each occupation pattern was found, which can vary from 2 to 13 hours depending on the occupation patterns' structure and the realistic range of initial values for water temperature in each pattern. Moreover, a simple guideline for finding these contract hour sets was suggested. The guideline helps the aggregator and end-user to generate a

wide range of contract hour sets conveniently, as it gives more options to choose from. The accuracy of the proposed approach in determining the maximum number of contract hours was also evaluated. Finally, a cost-benefit analysis was performed to investigate the minimum expected payment to end-users for covering the additional costs incurred to the summerhouse owner by proving flexibility services. Future directions for this work could be applying the method to other flexible devices or mix of devices in the buildings and including more complicated thermal loads in the model.

Acknowledgement

Appendix A. A brief review on backward scenario reduction method

We used the proposed backward scenario reduction method in [29] to decrease the system uncertainty scenarios. here we apply the approach to price uncertainty scenarios. however, it can be easily adapted to the ambient temperature and initial state scenarios too.

Let define $C^j = \{C_1^j, C_2^j, ...C_N^j\}$ as daily price scenario $j \in J$ with probability of ρ_j^p, where J is the set of all scenarios. The distance of each two scenarios C^j and C^l is defined as below:

$$DT(C^j, C^l) = \frac{1}{N}\sqrt{\sum_{k=1}^{N}(C_k^j - C_k^l)^2} \tag{A.1}$$

The process of reducing the price scenarios to n_p scenarios is explained as follows:

- **Step 1:** Compute the distance of all scenario pairs, i.e, $DT(C^j, C^l) \; \forall j, l \in J$.

- **Step 2:** For each scenario j, the scenario l_j^* which has the minimum distance with j, is identified.

- **Step 3:** Compute $PD_j = \rho_j^p \times DT(C^j, C^{l_j^*}) \; \forall j \in J$.

- **Step 4:** Find scenario d such that $PD_d = min\{PD_j \; \forall j \in J\}$.

- **Step 5:** $J = J - \{b\}$, $\rho_{l_b^*}^p = \rho_{l_b^*}^p + \rho_b^p$.

- **Step 6:** if $|J| > n_p$ ($|J|$ refers to cardinality of the set J), return to step 2, otherwise, stop the process.

References

[1] O. Babatunde, J. Munda, Y. Hamam, Power system flexibility: A review, Energy Reports 6 (2020) 101–106, the 6th International Conference on Power and Energy Systems Engineering. `doi:https://doi.org/10.1016/j.egyr.2019.11.048`. URL `https://www.sciencedirect.com/science/article/pii/S2352484719309242`

[2] F. D'Ettorre, M. Banaei, R. Ebrahimy, S. A. Pourmousavi, E. Blomgren, J. Kowalski, Z. Bohdanowicz, B. Łopaciuk Gonczaryk, C. Biele, H. Madsen, Exploiting demand-side flexibility: State-of-the-art, open issues and social perspective, Renewable and Sustainable Energy Reviews 165 (2022) 112605. `doi:https://doi.org/10.1016/j.rser.2022.112605`.

[3] M. Banaei, F. D'Ettorre, R. Ebrahimy, E. M. V. Blomgren, H. Madsen, Mutual impacts of procuring energy flexibility and equipment degradation at the residential consumers level, in: 2021 IEEE PES Innovative Smart Grid Technologies Europe (ISGT Europe), 2021, pp. 1–6. `doi:10.1109/ISGTEurope52324.2021.9640142`.

[4] P.-H. Li, S. Pye, Assessing the benefits of demand-side flexibility in residential and transport sectors from an integrated energy systems perspective, Applied Energy 228 (2018) 965–979. `doi:https://doi.org/10.1016/j.apenergy.2018.06.153`.

[5] M. Rossi, G. Viganò, H. Svendsen, G. Leclercq, P. Sels, M. Pavesi, T. Gueuning, J. Jimeno, N. Ruiz, C. Hermans, F. Spiessens, Y. Vardanyan, R. Ebrahimy, G. Howorth, Testing tso-dso interaction schemes for the participation of distribution energy resources in the balancing market - the smartnet simulator, in: The 25th International Conference and Exhibition on Electricity Distribution, 2019, pp. 1–5. `doi:10.5281/zenodo.3248777`.

[6] A. S. Gaur, D. Z. Fitiwi, J. Curtis, Heat pumps and our low-carbon future: A comprehensive review, Energy Research and Social Science 71 (2021) 101764. `doi:https://doi.org/10.1016/j.erss.2020.101764`.

[7] L. Schibuola, M. Scarpa, C. Tambani, Demand response management by means of heat pumps controlled via real time pricing, Energy and Buildings 90 (2015) 15–28. `doi:https://doi.org/10.1016/j.enbuild.2014.12.047`.

[8] L. Romero Rodríguez, J.S. Ramos, Servando, S. Álvarez Domínguez, and U. Eicker, Contributions of heat pumps to demand response: A case study of a plus-energy dwelling, Applied Energy 214 (2018. https://doi.org/10.1016/j.apenergy.2018.01.086) 191–204.

[9] X. Yuan, L. Lindroos, J. Jokisalo, R. Kosonen, Y. Pan, H. Jin, Demand response potential of district heating in a swimming hall in finland, Energy and Buildings 248 (2021) 111149. `doi:https://doi.org/10.1016/j.enbuild.2021.111149`.

[10] P. Fitzpatrick, F. D'Ettorre, M. De Rosa, M. Yadack, U. Eicker, D. P. Finn, Influence of electricity prices on energy flexibility of integrated hybrid heat pump and thermal storage systems in a residential building, Energy and Buildings 223 (2020) 110142. `doi:https://doi.org/10.1016/j.enbuild.2020.110142`.

[11] B. Baeten, F. Rogiers, L. Helsen, Reduction of heat pump induced peak electricity use and required generation capacity through thermal energy storage and demand response, Applied Energy 195 (2017. https://doi.org/10.1016/j.apenergy.2017.03.055) 184 – 195.

[12] D. Marini, R.A. Buswell, C.J. Hopfe, Sizing domestic air-source heat pump systems with thermal storage under varying electrical load shifting strategies, Applied Energy 255 (2019. https://doi.org/10.1016/j.apenergy.2019.113811) 113811.

[13] F.L. Müller and B. Jansen, Large-scale demonstration of precise demand response provided by residential heat pumps, Applied Energy 239 (2019. https://doi.org/10.1016/j.apenergy.2019.01.202) 836–845.

[14] T. Sweetnam, M. Fell, E. Oikonomou, and T. Oreszczyn, Domestic demand-side response with heat pumps: controls and tariffs, Building Research & Information (2018. https://doi.org/10.1080/09613218.2018.1442775).

[15] T. Péan, R. Costa-Castelló, E. Fuentes, J. Salom, Experimental testing of variable speed heat pump control strategies for enhancing energy flexibility in buildings, IEEE Access 7 (2019. DOI: 10.1109/ACCESS.2019.2903084) 37071–37087.

[16] E. Bee, A. Prada, and P. Baggio, Demand-Side Management of Air-Source Heat Pump and Photovoltaic Systems for Heating Applications in the Italian Context, Environments 5 (2018. https://doi.org/10.3390/environments5120132) 132.

[17] D. Fischer, T. R. Toral, K. Lindberg, B. Wille-Haussmann, H. Madani, Investigation of thermal storage operation strategies with heat pumps in german multi family houses, Energy Procedia 58 (2014) 137–144, renewable Energy Research Conference, RERC 2014. `doi:https://doi.org/10.1016/j.egypro.2014.10.420`.

[18] K. Leerbeck, P. Bacher, R.G. Junker, A. Tveit, O. Corradi, H. Madsen, R. Ebrahimy, Control of Heat Pumps with CO2 Emission Intensity Forecasts, Energies 13 (11) (2020).

[19] J. Rominger, F. Kern, H. Schmeck, Provision of frequency containment reserve with an aggregate of air handling units, Computer Science - Research and Development 33 (2018.) 215–221.

[20] L. Romero Rodríguez, M. Brennenstuhl, M. Yadack, P. Boch, U. Eicker, Heuristic optimization of clusters of heat pumps: A simulation and case study of residential frequency reserve, Applied Energy 233-234 (2019) 943–958. `doi:https://doi.org/10.1016/j.apenergy.2018.09.103`.

[21] Y.-J. Kim, L. K. Norford, J. L. Kirtley, Modeling and analysis of a variable speed heat pump for frequency regulation through direct load control, IEEE Transactions on Power Systems 30 (1) (2014) 397–408.

[22] A. Mufaris, S. Kawachi, J. Baba, Voltage control using coordinated control of heat pump water heaters with large penetration of photovoltaic systems, in: 2013 3rd International Conference on Electric Power and Energy Conversion Systems, IEEE, 2013, pp. 1–6.

[23] E. M. V. Blomgren, R. Ebrahimy, A. Pourmousavi Kani, J. Kloppenborg Moler, F. D'Ettorre, M. Banaei, H. Madsen, Behind-the-meter energy flexibility modelling for aggregator operation with a focus on uncertainty, in: 2021 IEEE PES Innovative Smart Grid Technologies Europe (ISGT Europe), 2021, pp. 1–6. `doi:10.1109/ISGTEurope52324.2021.9640146`.

[24] W. Kampel, B. Aas, A. Bruland, Energy-use in norwegian swimming halls, Energy and Buildings 59 (2013) 181–186. `doi:https://doi.org/10.1016/j.enbuild.2012.11.011`.
URL `https://www.sciencedirect.com/science/article/pii/S0378778812006007`

[25] J. C. Lam, W. W. Chan, Life cycle energy cost analysis of heat pump application for hotel swimming pools, Energy Conversion and Management 42 (11) (2001) 1299–1306. `doi:https://doi.org/10.1016/S0196-8904(00)00146-1`.
URL `https://www.sciencedirect.com/science/article/pii/S0196890400001461`

[26] smartnet project, `http://smartnet-project.eu/wp-content/uploads/2019/06/D7.7_20190621_V1.0.pdf`, accessed: 2022-05-20 (2021).

[27] T. Jónsson, P. Pinson, H. Madsen, H. A. Nielsen, Predictive densities for day-ahead electricity prices using time-adaptive quantile regression, Energies 7 (9) (2014) 5523–5547.

[28] P. Pinson, H. Madsen, H. A. Nielsen, G. Papaefthymiou, B. Klöckl, From probabilistic forecasts to statistical scenarios of short-term wind power production, Wind Energy 12 (1) (2009) 51–62. `doi:https://doi.org/10.1002/we.284`.

[29] L. Wu, M. Shahidehpour, T. Li, Stochastic security-constrained unit commitment, IEEE Transactions on Power Systems 22 (2) (2007) 800–811. `doi:10.1109/TPWRS.2007.894843`.

[30] N. Zemtsov, J. Hlava, G. Frantsuzova, H. Madsen, R. G. Junker, J. B. Jogensen, Economic mpc based on lpv model for thermostatically controlled loads, in: 2017 International Siberian Conference on Control and Communications (SIBCON), 2017, pp. 1–5. `doi:10.1109/SIBCON.2017.7998560`.